

## THE *SWIFT*/BAT HIGH-LATITUDE SURVEY: FIRST RESULTS

C. B. MARKWARDT,<sup>1,2</sup> J. TUELLER,<sup>2</sup> G. K. SKINNER,<sup>3</sup> N. GEHRELS,<sup>2</sup> S. D. BARTHELMY,<sup>2</sup> AND R. F. MUSHOTZKY<sup>4</sup>

Received 2005 August 15; accepted 2005 October 5; published 2005 October 28

### ABSTRACT

We present preliminary results from the first 3 months of the *Swift* Burst Alert Telescope (BAT) high Galactic latitude survey in the 14–195 keV band. The survey reaches a flux of  $\sim 10^{-11}$  ergs cm<sup>-2</sup> s<sup>-1</sup> and has  $\sim 2.7$  (90% confidence) positional uncertainties for the faintest sources. This represents the most sensitive survey to date in this energy band. These data confirm the conjectures that a high-energy-selected active galactic nucleus (AGN) sample would have very different properties from those selected in other bands and that it represents a “true” sample of the AGN population. We have identified 86% of the 66 high-latitude sources. Twelve are Galactic-type sources, and 44 can be identified with previously known AGNs. All but five of the AGNs have archival X-ray spectra, enabling us to estimate the line-of-sight column densities and other spectral properties. Both of the  $z > 0.11$  objects are blazars. The median redshift of the others (excluding radio-loud objects) is 0.012. We find that the column density distribution of these AGNs is bimodal, with 64% of the nonblazar sources having column densities  $N_{\text{H}} \geq 10^{22}$  cm<sup>-2</sup>. None of the sources with  $\log L_{\text{x}} > 43.5$  (cgs units) show high column densities, and very few of the lower  $L_{\text{x}}$  sources have low column densities. Based on these data, we expect the final BAT catalog to have  $> 200$  AGNs and reach fluxes of less than  $\sim 10^{-11}$  ergs cm<sup>-2</sup> s<sup>-1</sup> over the entire sky.

*Subject headings:* galaxies: active — gamma rays: observations — surveys

*Online material:* machine-readable table

### 1. INTRODUCTION

It is now realized that most active galactic nuclei (AGNs) have high column densities of absorbing material in our line of sight that significantly change their observable properties across much of the electromagnetic spectrum. This material can effectively hide the soft X-ray, optical, and UV signatures of an active nucleus. There are two spectral bands, the hard X-ray ( $E > 20$  keV) and the mid-IR (5–50  $\mu\text{m}$ ), where this obscuring material is relatively optically thin for column densities less than  $10^{24}$  cm<sup>-2</sup>. Thus, these bands are optimal for unbiased AGN searches (Treister & Urry 2005). Recent observations with the *Spitzer Space Telescope* are revealing many AGNs via their IR emission (Stern et al. 2005), but this process is hampered by strong emission from star formation and the lack of a unique spectral signature to separate AGNs from normal galaxies.

There has been little progress in hard X-ray surveys in the last 25 years due to a lack of instruments with sufficient angular resolution to identify counterparts in other wavelength bands or with sufficient sky coverage and sensitivity to produce a large sample. *INTEGRAL* observations are predominantly in the Galactic plane, and high-latitude coverage is patchy.

Here we report preliminary results from the *Swift* Burst Alert Telescope (BAT) high Galactic latitude ( $|b| > 19^\circ$ ) survey. Although this report is based on only the first 3 months, we detect 66 sources above  $5.5 \sigma$  significance. Only nine of the sources do not have firm identifications. Being basically unaffected by obscuration, BAT determines the intrinsic 14–195 keV luminosity,  $L_{\text{x}}$ . The survey is already about 10 times more sensitive than the previous large solid angle survey in this band from

*HEAO 1 A-4* (Levine et al. 1984) and covers the whole sky at  $\sim (1-3) \times 10^{-11}$  ergs cm<sup>-2</sup> s<sup>-1</sup>.

### 2. OBSERVATIONS

The BAT instrument on *Swift* is a very large field-of-view-coded aperture, hard X-ray telescope with a CdZnTe detector array ( $\sim \frac{1}{8}$  of the sky is at least partially coded at any one time). While primarily designed for the detection and rapid dissemination of gamma-ray burst positions, the BAT is also an effective all-sky hard X-ray monitor and survey instrument. The BAT focal plane consists of a 0.5 m<sup>2</sup> CdZnTe array, divided into 32,768 detectors, providing good sensitivity and energy resolution in the 14–195 keV energy range. BAT can reach  $\sim 65$  mcrab in a typical 450 s integration and typically covers 50%–80% of the sky each day. The effective exposure during the first 3 months varies over the sky from 200 to 800 ks. Away from the Galactic center region, the sensitivity scales as the square root of the exposure and so varies by a factor of 2 (Fig. 1). The statistical quality of the BAT survey map can be assessed by comparing positive and negative fluctuations. Figure 2 shows the excess in positive fluctuations of individual pixels. With the reconstruction algorithm used, each source appears in several correlated pixels; the source detection significance is approximately the peak value. Since the noise distribution is symmetric, and since there are no pixels  $< -5.5 \sigma$ , we expect no false detections above our  $+5.5 \sigma$  threshold. We estimate that the sensitivity limit is  $< 0.5$  mcrab for  $\sim 50\%$  of the sky.

The survey is based on individual sky images produced using fast Fourier transforms (FFTs) to correlate the detector data from one pointing (typically a few thousand seconds) with the mask pattern. The FFT is oversampled by a factor of 2 to prevent loss of sensitivity at bin boundaries. Each image is a tangent plane projection with a point-spread function (PSF) of 22' FWHM at the image center. A single image has very nonuniform sensitivity due to partial coding at the edges (we exclude regions with  $< 15\%$  partial coding). Background variations around the orbit and other systematic effects cause the noise to vary both spatially and temporally. To achieve a good sensitivity, it is necessary to clean

<sup>1</sup> Department of Astronomy, University of Maryland, College Park, MD 20742; craigm@milkyway.gsfc.nasa.gov.

<sup>2</sup> Astroparticle Physics Laboratory, Mail Code 661, NASA Goddard Space Flight Center, Greenbelt, MD 20771.

<sup>3</sup> Centre d'Etude Spatiale des Rayonnements, CNRS/UPS, 9 Avenue du Colonel Roche, 31028 Toulouse Cedex 04, France.

<sup>4</sup> X-Ray Astrophysics Laboratory, Mail Code 662, NASA Goddard Space Flight Center, Greenbelt, MD 20771.

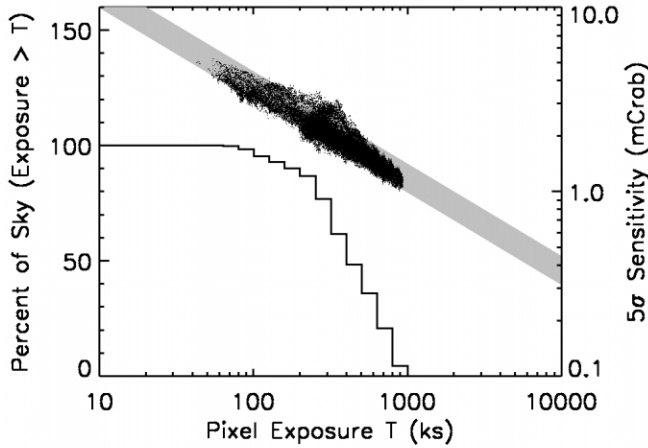


FIG. 1.—BAT all-sky sensitivity and exposure statistics. Dots (*top*; right scale) represent the  $5\sigma$  pixel sensitivity threshold. The gray band corresponds to the function  $8.5 \pm 1.5 \text{ mcrab } (T/20 \text{ ks})^{-0.5}$ , extrapolated to larger exposures  $T$ . The solid line (*bottom*; left scale) is the cumulative sky coverage with an exposure of greater than  $T$ , expressed as a percentage of the solid angle analyzed ( $100\% = 0.67 \times 4\pi$ ).

from the data the effects of bright sources and of constant background nonuniformities. The noise in the resulting cleaned images is often near the statistical limit. However, some excess noise remains, so uncertainties used in this analysis are calculated from the observed rms noise in the images. These images are interpolated and combined to form an all-sky map with  $5'$  sampling. Pixel weights are based on the local rms noise in the component images. The rms error is then recalculated, and the image is searched for local maxima greater than  $5.5\sigma$ . Each maximum is least-squares-fitted with a Gaussian PSF to derive a position and flux.

The output from two separate analysis pipelines (one developed by authors C. B. M. and J. T. and the other by G. K. S.), using somewhat different background correction and image combination algorithms, have been compared, and they agree well.

Figure 2 shows the BAT confidence contours plotted on the images of two known sources, illustrating the variation in position accuracy with source significance. The systematic and statistical errors are estimated by comparing  $\sim 1800$  BAT position measurements with the known positions for  $\sim 60$  X-ray sources. The precision improves from  $\sim 3.7'$  (95% confidence radius) for sources at  $\sim 6\sigma$  significance to  $\sim 0.9'$  at  $>20\sigma$  significance. For these early data, the flux calibration is uncertain by  $\sim 30\%$  as a result of the spectrally dependent count rate-to-flux conversion.

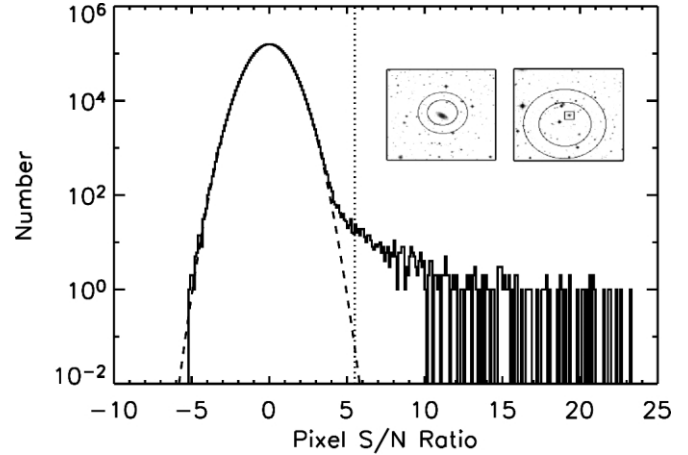


FIG. 2.—Distribution of BAT all-sky map pixel significances. The best-fit Gaussian curve (*dashed curve*) has a mean and standard deviation of 0.002 and 1.009, respectively. The vertical dotted line is the pixel-detection threshold of  $5.5\sigma$ . *Insets*: Example BAT-detected sources overlaid on DSS images centered on MCG  $-5-23-016$  (*left*) and 3C 390.3 (*right*), respectively. The images are  $8'$  on a side (east is left, north is up). The larger circles represent the BAT 90% and 99% confidence regions for significances of  $26\sigma$  (MCG  $-5-23-016$ ) and  $10\sigma$  (3C 390.3). The small box identifies 3C 390.3.

At present, the calculation of exposure as a function of sky position is still approximate. Consideration of the  $\log N$ - $\log S$  distribution and of source spectra are thus left to a later paper.

### 3. RESULTS

Our list contains 66 sources at  $|b| > 19^\circ$ , of which 12 can be identified as Galactic or SMC/LMC objects, and 45 have clear identifications with cataloged optical objects (see, e.g., the catalog of Veron-Cetty & Veron 2003). Except for the Coma Cluster, all 45 are known AGNs (Table 1). Of the nine remaining detections, we have tentative identifications for four cataloged objects that do not have bright *ROSAT* counterparts. Two of the unidentified detections are *RXTE* slew survey sources (XSS J05054-2348 and XSS J12389-1614, which have nearby bright galaxies). Three sources do not have obvious optical counterparts. All but five of the cataloged AGNs (ESO 297-018, NGC 1142, MCG +04-22-042, ESO 323-077, and Mrk 1498) have published or available X-ray spectra.

The identified sources are dominated by low-luminosity, low-redshift objects. There are three blazars (3C 273, 4C +71.07, and Mrk 421) and five radio-loud AGNs (3C 390.3, Cen A, 3C 120, 4C +74.26, and Mrk 1498), consistent with the roughly

TABLE 1  
BAT DETECTIONS OF AGNs

<i>Swift</i> Name	R.A. (J2000) (deg)	Decl. (J2000) (deg)	Err. <sup>a</sup> (arcmin)	Identification	Offset (arcmin)	$z$	$\log N_{\text{H}}$ ( $\text{cm}^{-2}$ )	Ref.	$\log L_{\text{X}}^{\text{b,c,d}}$ ( $\text{ergs s}^{-1} \text{cm}^{-2}$ )	RL <sup>e</sup>	Type <sup>f</sup>
J0048.8+3157 .....	12.200	31.963	4.8	Mrk 348	0.4	0.0150	22.9	1	43.7	N	Sy

NOTE.—Table 1 is published in its entirety in the electronic edition of the *Astrophysical Journal*. A portion is shown here for guidance regarding its form and content.

<sup>a</sup> Error radius (99% confidence).

<sup>b</sup> BAT luminosity, 14–195 keV.

<sup>c</sup> Estimated systematic error: +20%, –50%.

<sup>d</sup> Assumes a *WMAP* cosmology ( $H_0 = 71 \text{ km s}^{-1} \text{ Mpc}^{-1}$ ,  $\Omega_M = 0.27$ ,  $\Omega_\Lambda = 0.73$ ; Spergel et al. 2003).

<sup>e</sup> Radio-loud? N = no; Y = yes.

<sup>f</sup> Sy = Seyfert; Bl = blazar.

REFERENCES.—(1) Turner et al. 2001; (2) Lutz et al. 2004; (3) this work (*XMM-Newton*); (4) Gilli et al. 2000; (5) this work (*ASCA*); (6) Gondoin et al. 2003; (7) Vignali & Comastri 2002; (8) Perlman et al. 2005; (9) this work (*Chandra*).

10% of all AGNs that are thought to be radio-loud. The line-of-sight column densities and X-ray fluxes of the 39 objects (three blazars and 36 Seyfert galaxies) with X-ray spectra have been obtained primarily by *ASCA* or *BeppoSAX* (e.g., Lutz et al. 2004). In those cases for which Lutz et al. do not quote a column density, we have used results from the Tartarus *ASCA* database or from archival *XMM-Newton* or *Chandra* data. Because the Tartarus database uses only simple spectral models, the precision of column densities is only  $\pm 0.5$  dex. However, this is sufficient to categorize whether the objects as heavily absorbed or not.

Assuming a typical power-law spectrum ( $\Gamma \sim 1.7$ ), a conservative absorption column ( $\log N_{\text{H}} = 24$ ), and the BAT limiting flux, we derive a 2–10 keV limiting flux of  $\sim 10^{-12}$  ergs  $\text{cm}^{-2} \text{s}^{-1}$ . Using the flux distribution of Moretti et al. (2003), we expect  $< 0.01$  chance sources per BAT error circle, and hence  $< 1$  misidentification overall.

Excluding the blazars, the median redshift is  $z \sim 0.012$  (the mean is 0.018), giving a median  $\log L_{\text{X}} = 43.3$  in the 14–195 keV band and a median column density of  $\log N_{\text{H}} = 22.6$ . The X-ray luminosity versus column density scatter plot for the nonblazars (Fig. 3) shows an absence of high column density, highly luminous sources.

A surprising result from our survey is the very high fraction of identified sources. In *HEAO 1* (Piccinotti et al. 1982), approximately half of the 2–10 keV X-ray-selected AGNs were “new” objects. In the deep *Chandra* surveys (Barger et al. 2005), approximately a third of all sources did not show a strong optical AGN signature. We thus anticipated that many of the BAT hard X-ray-selected objects would not have a cataloged AGN counterpart. The high identification rate of this first BAT sample shows that, contrary to some suggestions, classical optical techniques have been successful at finding objects with high line-of-sight column densities in the low-redshift universe.

Defining an absorbed object as one with  $\log N_{\text{H}} \geq 22.0$  (Ueda et al. 2003), the ratio of absorbed to unabsorbed objects is 1.8:1 (excluding the blazars), somewhat less than suggested by the standard “unified” AGN models. The distribution of column densities is approximately bimodal (Fig. 3). The fact that a ratio of 1:3 was found by Sazonov & Revnivtsev (2004) for identified sources in the *RXTE* slew survey indicates the strength of the bias toward the detection of unabsorbed objects in 2–10 keV low-redshift X-ray surveys.

The distribution of optical classes of the BAT sources is very different from those in an optical color-selected or line-selected survey, with only 20% of the objects being optically classified as Seyfert I galaxies, compared with  $\sim 40\%$  in optical surveys at low redshift. This illustrates the power of a hard X-ray survey to find all classes of AGNs.

Given the limited sensitivity of the BAT survey (all but 15% of the sources are brighter than  $\sim 3 \times 10^{-11}$  ergs  $\text{cm}^{-2} \text{s}^{-1}$ ), it is surprising that many are not in the *HEAO 1* A-2 catalog (Piccinotti et al. 1982). Most of the 18 objects not seen by *HEAO 1* were clearly missed due to obscuration, since 12 of them have column densities greater than  $10^{23} \text{ cm}^{-2}$ . Three of these “missing” objects (Ark 120, 3C 390.3, and 4C +74.26) are known to be highly variable.

Comparison of the *HEAO 1* 2–10 keV fluxes with the more recent *RXTE* fluxes (Revnivtsev et al. 2004) shows a variation of  $\sim 60\%$  in flux, with only  $\sim 10\%$  of the objects showing more than a factor of 2 variability across the  $\sim 20$  years between these two data sets. While the *RXTE* slew survey is much more sensitive than BAT for unabsorbed objects, at least eight BAT

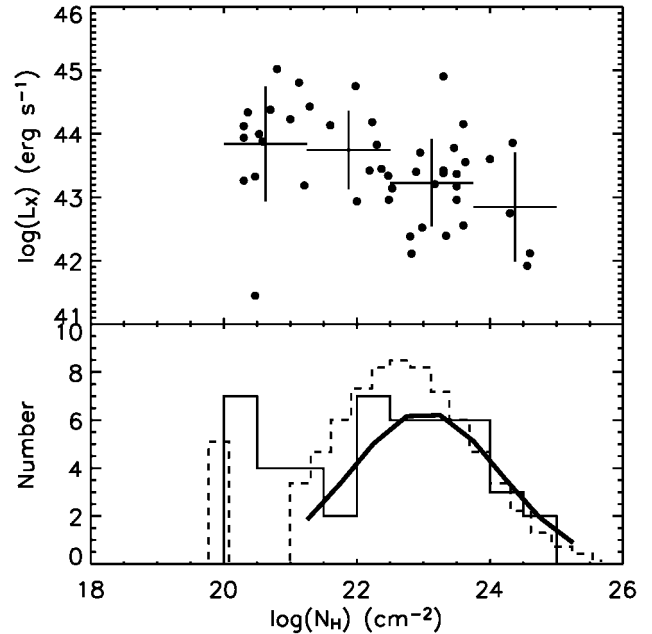


FIG. 3.—Correlation between absorption and BAT hard X-ray luminosity (filled circles; top). The crosses show the mean and standard deviations of the luminosity in several  $N_{\text{H}}$  bins. The distribution of absorptions for BAT-detected sources is shown in the bottom panel (solid line). Also shown are the distribution predicted by Hopkins et al. (2005a) (dashed histogram) and a Gaussian fit to the bins for  $\log N_{\text{H}} > 21$  (solid histogram; centroid = 23.0;  $\sigma = 1.1$ ). The peaks at  $\log N_{\text{H}} \sim 20$ –21 are artificial: for the BAT sources, the peak is an upper limit to the measurable absorption in the 2–10 keV band; Hopkins et al. collect all sources for  $\log N_{\text{H}} < 21$  into a single bin.

sources were not detected in the *RXTE* data (Mrk 348, Mrk 1498, NGC 3081, UGC 5037, NGC 1142, and NGC 1365). Of these, three have high column densities, and three do not have X-ray spectra.

Most (36/44) of the AGNs have cataloged *ROSAT* fluxes (taken from the ROSPSPC catalog when available, otherwise taken from the *ROSAT* All-Sky Survey database). There is little or no correlation between the BAT and *ROSAT* fluxes. This is not surprising because the scatter in the *ROSAT* rates is dominated by the effect of different degrees of intrinsic absorption in the sources, whereas these have relatively little effect in the BAT energy range. This illustrates the difficulty of constructing a complete AGN sample from soft X-ray data. Since there is a very strong relation between optical nuclear and soft X-ray flux (Mushotzky 2004; Barger et al. 2005), samples based on optical data are subject to similar difficulties.

A crucial component for models of the X-ray background is the distribution of  $N_{\text{H}}$  values. Our data determine this distribution, in an unbiased way, for the first time. There is little evidence for variation of  $N_{\text{H}}$  with  $L_{\text{X}}$  below  $\log L_{\text{X}} = 43.5$ , but above this luminosity,  $\langle \log N_{\text{H}} \rangle$  drops to  $\sim 20.9$  compared with 22.9 below it. This break point occurs around the characteristic luminosity of AGNs in the *Chandra* surveys of  $\log L_{\text{X}} \sim 43.8$  (corrected for the bandpass differences; Barger et al. 2005) and is probably related to this feature. The only object at  $\log L_{\text{X}} > 43.5$  with a high line-of-sight column density is EXO 055620–3820.2. This object (Crenshaw & Kraemer 2001) has complex absorbing material (Quadrelli et al. 2003) that seems to be associated with the host galaxy. In the entire BAT AGN sample, including low-latitude objects, there are no extragalactic objects with  $\log L_{\text{X}} <$

42.5 that are not heavily absorbed. This is not a selection effect. While such objects clearly exist (e.g., NGC 3998; Ptak et al. 2004), they must be rare. The BAT data establish the  $z = 0$  relationship of absorption and luminosity needed to model the evolution of hard X-ray sources (e.g., Mateos et al. 2005).

Recently, Hopkins et al. (2005a, 2005b) have constructed physical models that apparently can explain much of the observed evolution of AGNs and the differences between samples in different wavelength bands. These models only correctly predict the observed absorption distribution when they include cold material in the line of sight. The predicted distribution of column densities and the predicted loose correlation between  $L_x$  and  $N_H$  are in rough agreement with the BAT data. However, this model completely misses the observed sharp reduction in high  $N_H$  objects at high luminosity.

Comparing the BAT luminosities with 3.5 or 10  $\mu\text{m}$  IR luminosities (e.g., Lutz et al. 2004; Gorjian et al. 2004) shows little or no correlation. A similar lack of correlation of the IR-to-BAT flux ratios with X-ray absorption indicates a wide scatter between observed IR properties and the intrinsic properties of AGNs. Previous work (Krabbe et al. 2001) had reported a strong correlation between the 10  $\mu\text{m}$  IR fluxes and the hard X-ray fluxes, naïvely expected if the near-IR is dominated by AGN light that is relatively unabsorbed. However, in the new *Spitzer* results (Franceschini et al. 2005), such a correlation is only seen for type I objects. This lack of correlation may be due to additional IR radiation from star formation, high optical depths even at 10  $\mu\text{m}$ , or additional scatter introduced by reprocessing of the nuclear radiation in the IR. The absence of a correlation makes the analysis using the unified models to connect the IR and X-ray data suspect (Treister & Urry 2005). Similarly there is little or no correlation between BAT and [O III] luminosities.

The BAT sample allows a true measure of the nature of the low- $z$  hosts of active galaxies. Of the 24 objects in the sample with “T” types as categorized in the Third Reference Catalogue of Bright Galaxies (de Vaucouleurs et al. 1991), nine have T types  $< 0$ , indicating a spheroidal host fraction of  $\sim 40\%$ , similar to that seen in the *Chandra* surveys and the SDSS data (Kauffmann & Heckman 2005; Grogin et al. 2005). This is much larger than the fraction in classical optical surveys. However, none of the objects is classified as a giant elliptical galaxy,

which is rather different than the results of *Chandra* surveys, probably due to the low redshifts probed by the BAT sample.

It is interesting to note that all the broad-line radio galaxies detected by *HEAO 1* (Marshall et al. 1979; 3C 111.0, 3C 120, 3C 382, and 3C 390.3) are detected by the BAT, indicating that radio galaxies may have systematically harder X-ray spectra in the BAT band than Seyfert galaxies.

#### 4. CONCLUSIONS

We have shown the usefulness of a sensitive, large solid angle hard X-ray survey in defining the nature of the AGN population. As predicted by models of the X-ray background, the dominant source populations are absorbed AGNs, which are very different from an optically or soft X-ray–derived AGN population. We derive the true distribution of the absorbing column density with X-ray luminosity and find that while virtually all sources with  $\log L_x < 43.5$  are absorbed, those with higher luminosities are mostly unabsorbed. This luminosity corresponds to the break in the X-ray luminosity function and is a strong clue to the nature of the absorbing material and the origin of the feature in the luminosity function. We find little correlation between other measures of the luminosity of absorbed AGNs (e.g., [O III], 3.5 or 10  $\mu\text{m}$  luminosity) and the hard X-ray luminosity, suggesting that previous techniques may have unsuspected biases in finding and measuring absorbed AGNs. The high identification fraction ( $\sim 86\%$ ) is somewhat unexpected given our previous knowledge of these sources and bodes well for the much larger samples that the BAT will obtain over the next 2 years.

Further work on the present sample will include determination of the  $\log N$ – $\log S$  of the hard X-ray sample, the luminosity function, and spectral and temporal analysis of the BAT-selected AGNs directed toward a detailed understanding of the relationship of the hard X-ray to other wavelength bands. Preliminary estimates indicate that an eventual 3(+) $\text{yr}$  BAT high-latitude catalog will have more than 200 AGNs, which will allow us to make extensive correlation analyses.

We thank the BAT and *Swift* teams for their extensive efforts, which have made this work possible.

#### REFERENCES

- Barger, A. J., Cowie, L. L., Mushotzky, R. F., Yang, Y., Wang, W.-H., Steffen, A. T., & Capak, P. 2005, *AJ*, 129, 578
- Crenshaw, D. M., & Kraemer, S. B. 2001, *ApJ*, 562, L29
- de Vaucouleurs, G., de Vaucouleurs, A., Corwin, H. G., Jr., Buta, R. J., Paturel, G., & Fouqué, P. 1991, *Third Reference Catalogue of Bright Galaxies* (New York: Springer)
- Franceschini, A., et al. 2005, *AJ*, 129, 2074
- Gilli, R., Maiolino, R., Marconi, A., Risaliti, G., Dadina, M., Weaver, K. A., & Colbert, E. J. M. 2000, *A&A*, 355, 485
- Gondoin, P., Orr, A., Lumb, D., & Siddiqui, H. 2003, *A&A*, 397, 883
- Gorjian, V., Werner, M. W., Jarrett, T. H., Cole, D. M., & Ressler, M. E. 2004, *ApJ*, 605, 156
- Grogin, N. A., et al. 2005, *ApJ*, 627, L97
- Hopkins, P. F., Hernquist, L., Cox, T. J., Di Matteo, T., Robertson, B., & Springel, V. 2005a, *ApJ*, submitted (astro-ph/0506398)
- Hopkins, P. F., Hernquist, L., Cox, T. J., Robertson, B., & Springel, V. 2005b, *ApJ*, submitted (astro-ph/0508167)
- Kauffmann, G., & Heckman, T. M. 2005, *Philos. Trans. R. Soc. London*, A363, 621
- Krabbe, A., Böker, T., & Maiolino, R. 2001, *ApJ*, 557, 626
- Levine, A., et al. 1984, *ApJS*, 54, 581
- Lutz, D., Maiolino, R., Spoon, H. W. W., & Moorwood, A. F. M. 2004, *A&A*, 418, 465
- Marshall, F. E., Boldt, E. A., Holt, S. S., Mushotzky, R. F., Rothschild, R. E., Serlemitsos, P. J., & Pravdo, S. H. 1979, *ApJS*, 40, 657
- Mateos, S., et al. 2005, *A&A*, 433, 855
- Moretti, A., Campana, S., Lazzati, D., & Tagliaferri, G. 2003, *ApJ*, 588, 696
- Mushotzky, R. 2004, in *Supermassive Black Holes in the Distant Universe*, ed. A. J. Barger (Dordrecht: Kluwer), 53
- Perlman, E. S., et al. 2005, *ApJ*, 625, 727
- Piccinotti, G., Mushotzky, R. F., Boldt, E. A., Holt, S. S., Marshall, F. E., Serlemitsos, P. J., & Shafer, R. A. 1982, *ApJ*, 253, 485
- Ptak, A., Terashima, Y., Ho, L. C., & Quataert, E. 2004, *ApJ*, 606, 173
- Quadrelli, A., Malizia, A., Bassani, L., & Malaguti, G. 2003, *A&A*, 411, 77
- Revnivtsev, M., Sazonov, S., Jahoda, K., & Gilfanov, M. 2004, *A&A*, 418, 927
- Sazonov, S. Yu., & Revnivtsev, M. G. 2004, *A&A*, 423, 469
- Spergel, D. N., et al. 2003, *ApJS*, 148, 175
- Stern, D., et al. 2005, *ApJ*, 631, 163
- Treister, E., & Urry, C. M. 2005, *ApJ*, 630, 115
- Turner, T. J., Nandra, K., Turcan, D., & George, I. M. 2001, in *AIP Conf. Proc. 599, X-Ray Astronomy: Stellar Endpoints, AGN, and the Diffuse X-Ray Background*, ed. N. E. White, G. Malaguti, & G. G. C. Palumbo (Melville: AIP), 991
- Ueda, Y., Akiyama, M., Ohta, K., & Miyaji, T. 2003, *ApJ*, 598, 886
- Veron-Cetty, M.-P., & Veron, P. 2003, *A&A*, 412, 399
- Vignali, C., & Comastri, A. 2002, *A&A*, 381, 834